Journal of Solid State Chemistry 182 (2009) 2225–2230

Contents lists available at ScienceDirect

Journal of Solid State Chemistry

journal homepage: www.elsevier.com/locate/jssc

The evolvement of pits and dislocations on TiO_2-B nanowires via oriented attachment growth

Bin Zhao, Feng Chen *, Wenwu Qu, Jinlong Zhang

Laboratory for Advanced Materials and Institute of Fine Chemicals, East China University of Science and Technology, 130 Meilong Road, Shanghai CA 200237, PR China

ARTICLE INFO

Article history:
Received 16 March 2009
Received in revised form
4 June 2009
Accepted 7 June 2009
Available online 12 June 2009

Keywords:
Titanium dioxide
One-dimensional nanomaterials
Thermal treatment
Phase transition
Growth mechanism

ABSTRACT

TiO_2-B nanowires were synthesized by an ion exchanging-thermal treatment. The unique morphology of pits and dislocations interspersed on TiO_2-B nanowires were firstly characterized and studied by high-resolution transmission electron microscopy (HRTEM). Oriented attachment is suggested as an important growth mechanism in the evolvement of pits and dislocations on TiO_2-B nanowires. Lattice shears and fractures were originally formed during the ion exchanging process of the sodium titanate nanowires, which resulted in the formation of primary crystalline units and vacancies in the layered hydrogen titanate nanowires. Then the (110) lattice planes of TiO_2-B grown in [110] direction is faster than the other lattice planes, which caused the exhibition of long dislocations on TiO_2-B nanowires. The enlargement of the vacancies, which was caused by the rearrangement of primary crystalline units, should be the reason of the formation of pits. Additionally, the transformation from TiO_2-B to anatase could be also elucidated by oriented attachment mechanism.

1. Introduction

One-dimensional (1D) nanostructured materials, such as nanowires and nanotubes, are particularly significant due to their superior physicochemical properties, such as superexcellent electronic, magnetic, optical, catalytic, and mechanical properties [1–5]. Of such materials, titania nanowires have received a great deal of attention because of their important photovoltaic (solar energy conversion), photocatalytic and gas-sensing properties [6–9]. Recently, the first synthesis of TiO_2-B nanowires by a hydrothermal route was reported [10,11]. TiO_2-B is the least dense polymorph of titania and the metastable monoclinic modification of titanium dioxide with a shear-derivative of the ReO_3 type structure. The structure of TiO_2-B is more open than other polymorphs, which makes TiO_2-B a more excellent host for intercalation [10,12]. Additionally, TiO_2-B nanowire has higher capability of lithium intercalation than bulk TiO_2-B as an anode material [11].

The transformation from titanate to TiO_2-B has been investigated by thermal analysis and crystallographic techniques, indicating that it is not a simple endothermic condensation of interlayer hydroxy groups, and involves an exothermic nucleation and growth step, which results in the formation of a TiO_2-B like intermediate, and the final TiO_2-B is formed by a low energy transformation [12]. Previous work also reveals that titanate nanowire will be fractionized into small single crystalline grains in more rigorous conditions [13]. Moreover, the growth mechanism of TiO_2-B film has demonstrated that the (0*k*0) planes of TiO_2-B were derived from the *a*-axis orientation of hydrogen titanate [14].

However, in the transformation from layered titanate to TiO_2-B nanowire how single crystal (or pseudo-single crystal) TiO_2-B nanowires with the length of several micrometers can be obtained from layered titanate nanowires is still mysterious. In recent years, oriented attachment has caught much attention in the research field of complex crystal growth and transformation [15–20]. As a novel and attractive growth mechanism, the characteristic of oriented attachment is that the primal units aggregate and orient along a certain direction to form secondary single crystalline structures, which was proposed and demonstrated firstly by Penn and Banfield in their work of iron oxyhydroxide and anatase (TiO_2) [15,16]. After that, many attempts have been made to demonstrate the oriented attachment in different materials [17–20].

In this contribution, TiO_2-B nanowires were synthesized by an ion exchanging-thermal treatment. The unique morphologies of pits and dislocations on TiO_2-B nanowires were firstly observed and studied with the assistance of high-resolution transmission electron microscopy (HRTEM), which revealed that the phase transformation was more complex and partly different from the reported hypothesis. The evolvement of pits and dislocations on TiO_2-B nanowires could be elucidated by oriented attachment

* Corresponding author. Fax: +86 21 64252062.
E-mail address: Fengchen@ecust.edu.cn (F. Chen).

0022-4596/$ - see front matter © 2009 Elsevier Inc. All rights reserved.
doi:10.1016/j.jssc.2009.06.008

mechanism. Consequently, the paper also gave a further reasonable explanation that how pseudo-single crystal TiO_2-B nanowires were grown from layered hydrogen titanate nanowires.

2. Experimental

2.1. Synthesis

Hydrogen titanate nanowires were synthesized by an alkaline solvothermal-ion exchanging treatment. In a typical procedure, TiO_2 (Degussa P25, which consists of about 30% rutile and 70% anatase and a particle size of about 30 nm) was dripped into a 10 M aqueous solution of NaOH under vigorous stirring. After being continuously stirred for 2 h at room temperature, the resulting suspension was transferred to a Teflon-lined autoclave and heated to 180 °C for 48 h. Then the product was acid-washed, which involved stirring the sample in 0.1 M HCl solution for 8–12 h in order to remove the residual Na^+ ion completely. The material was then filtered, washed with distilled water, and dried at 80 °C for 12 h.

TiO_2-B nanowires were finally prepared by heating the acid-washed product at 400 °C for 4 h in air. As compared, the acid-washed product was also calcined at 200, 500, 600, 800 and 1000 °C for 4 h in air, respectively.

2.2. Characterization

XRD patterns were obtained using a powder diffractometer (RIGAKU D/max2550) operating in the reflection mode with Cu$K\alpha$ radiation at a scan rate of $0.02^\circ\ 2\theta\ s^{-1}$. The average sizes of TiO_2-B and anatase crystallites were estimated from the half-peak widths at half the height of the diffraction peaks from the (110) plane of TiO_2-B ($2\theta = 24.9^\circ$) and from the (101) plane of anatase ($2\theta = 25.3^\circ$), respectively, using Scherrer equation.

The morphology of the collected powders was investigated using a high-resolution transmission electron microscopy (HRTEM, JEOL JEM-2100F) operated at 200 kV and equipped with EDX facilities. To prepare the HRTEM specimens, the powder samples were first dispersed ultrasonically in acetone. One drop of the suspension was placed on a carbon film supported on a copper grid and allowed to dry in air before the specimens were transferred into the microscope.

Specific surface areas were determined using an ASAP 2020 Micromeritics apparatus following the BET analysis. Adsorption and desorption of N_2 were performed at −196 °C. Samples had been previously outgassed by heating at 100 °C under vacuum (3 mm Hg).

3. Results and discussion

3.1. X-ray diffraction

The structural and morphological transformation of TiO_2-B nanowires were characterized by XRD and TEM, respectively. XRD patterns of sodium titanate, acid-washed titanate and the calcined samples are shown in Fig. 1. Fig. 1a gives a normal XRD pattern of sodium titanate $Na_2Ti_xO_{2x+1}$, probably $Na_2Ti_4O_9$. After H^+ ion-exchange, the most intense peak of the titanate structure at $2\theta \approx 10^\circ$ shifts to high-angle (Fig. 1b), suggesting that the layer spaces of titanates were narrowed as a result of the interlayered Na^+ ions replaced by hydroniums (H_3O^+ ions), which have stronger electrostatic interaction and polarization potential than the former. The structure of acid-washed product was identified as the layered hydrogen titanate $H_2Ti_xO_{2x+1}$, possibly $H_2Ti_4O_9$ or $H_2Ti_3O_7$ [21].

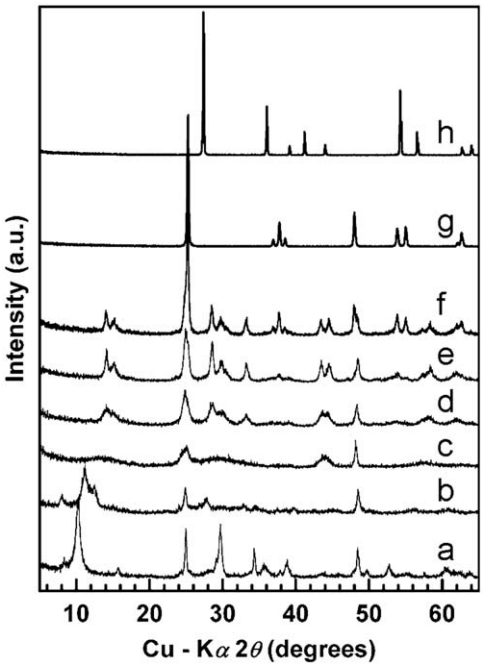

Fig. 1. XRD patterns of the titanate (a), hydrogen titanate (b), and the calcined samples for 4 h at 200 °C (c), 400 °C (d), 500 °C (e), 600 °C (f), 800 °C (g) and 1000 °C (h), respectively.

Layered hydrogen titanate would be dehydrated and start to transform crystal phase from 140 °C, which has been indicated by Yoshida with thermogravimetry-differential thermal analysis (TG-DTA) [22]. Fig. 1c presents two new broad peaks formed at $2\theta \approx 28$–32° and 43–45°, which matches the pattern for TiO_2-B, indicating the collapse of layered structures of hydrogen titanates at 200 °C and the appearance of TiO_2-B [23,24].

Layered hydrogen titanates would be converted to different titanium dioxide polymorphs in corresponding different conditions [10,22,24]. Although the diffraction peaks (Fig. 1d) associated with the nanowires obtained in the typical procedure (400 °C) are somewhat broadened due to dimensional confinement, the 2θ values of 14.12°, 24.86°, 28.64° and 48.34° correspond well to the (001), (110), (002) and (020) lattice planes of TiO_2-B [25,26].

Fig. 1e presents a new little peak formed at 2θ values of 37.64°, which matches the (004) lattice planes of anatase, indicating the transformation from TiO_2-B to anatase were started at 500 °C. The obvious diffraction peaks at 25.22°, 36.86°, 37.72°, 38.64° presented in Fig. 1f, which correspond to the (101), (103), (004), (112) lattice planes of anatase, indicate the coexistence of TiO_2-B and anatase at 600 °C and the further development of phase transformation. Fig. 1g gives a normal XRD pattern of anatase, which means a thorough transformation from TiO_2-B to anatase at 800 °C. Finally, Fig. 1h shows sample calcined at 1000 °C was pure rutile.

3.2. TEM images

TEM images in Fig. 2 show the diameter and length change of the nanowires with the increase in heating temperatures. Fig. 2a shows the ultralong hydrogen titanate nanowires with the length of several micrometers and diameter of about 50 nm. Nanowires tend to form bundles, thus some of the nanowires seem thicker than others. Sample calcined at 200 °C (Fig. 2b) is also ultralong nanowire, and the diameter of single nanowire changes little.

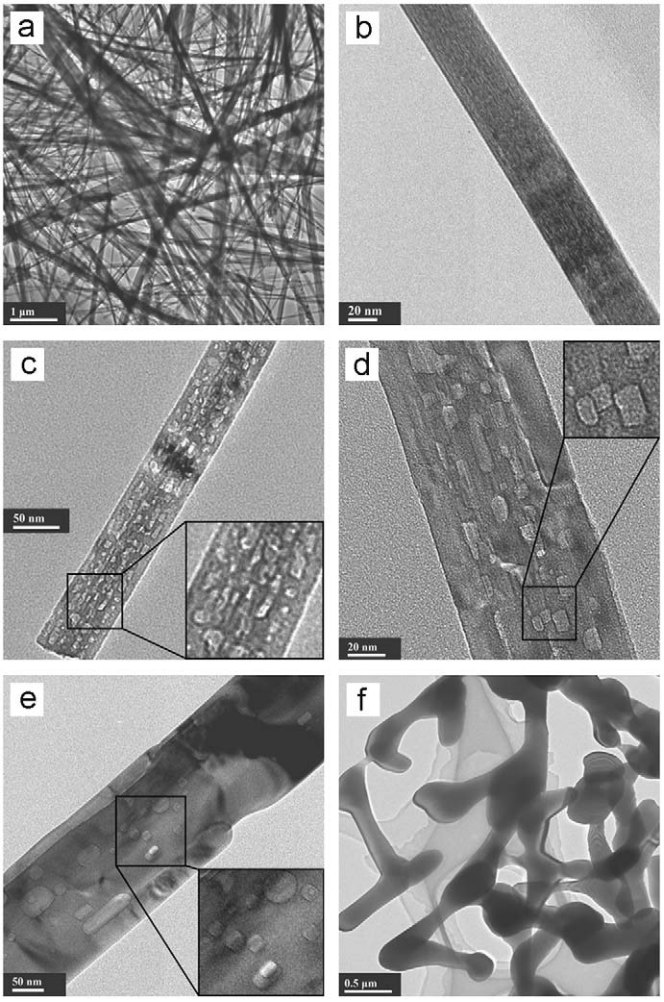

Fig. 2. TEM images of the acid-washed titanate nanowires (a) and nanowires calcined at 200 °C (b), 400 °C (c), 600 °C (d), 800 °C (e) and 1000 °C (f).

Nanowire obtained at 400 °C (Fig. 2c) gives a similar size (diameter of about 50 nm) as those of the hydrogen titanate nanowires and the sample calcined at 200 °C, which means no obvious size growth occurred till 400 °C. However, it is worthwhile to note that a great deal of pits with the pore size of 3–10 nm is presented throughout the surface of nanowires.

Samples calcined at 600 °C (Fig. 2d) also maintain the unique morphologies of pits in mesoscale, but the pore size of such pits is much larger than those of 200 and 400 °C samples. Take care that the diameter of single nanowire almost keeps no change, which means the enlargement of pits was not due to the growth of the nanowires, but probably the rearrangement of the pits themselves. Samples at 800 °C (Fig. 2e) maintain 1D structure, but fewer nanopits are found in the solid nanowires, which suggests a more rigorous rearrangement of pits had been undertaken in the process of phase transformation. The diameter of nanowires is more than 100 nm, indicating that a size growth of the nanowires occurred at 800 °C. Finally, nanowires calcined at 1000 °C (Fig. 2f) show submicron rod-like structure of rutile.

3.3. HRTEM images and mechanism discussion

TEM images of calcined nanowires from 400 to 800 °C indicate the unique pits on nanowires increased in size and decreased in amount. The HRTEM images in Figs. 3–5 give a further

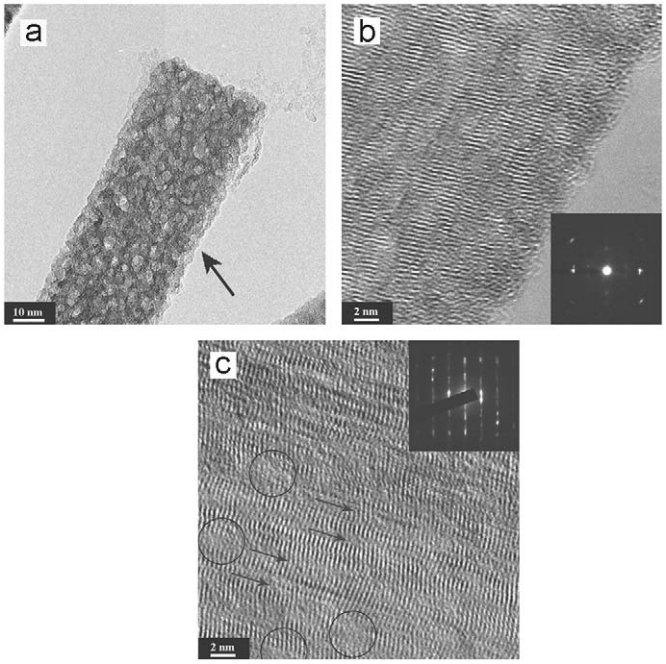

Fig. 3. HRTEM images of (a) hydrogen titanate nanowire in precise focus, (b) the further magnified region near arrow in Fig. 3a (inset: the corresponding SAED pattern), (c) nanowires calcined at 200 °C (inset: the corresponding SAED pattern).

demonstration of the growth mechanism of TiO_2-B nanowires. Fig. 3a shows a HRTEM image of hydrogen titanate nanowire recorded in precise focus, indicating that nanowires are fractionized into a great number of the primary crystalline units. Many small cracks are interspersed among such units. Regions arrowed in Fig. 3a are further magnified in Fig. 3b, which gives a clearer view of the single crystalline units with an average size of about 3–5 nm. The widespread vacancies between the primary crystallites, namely the intercrystalline areas, show few lattice planes in the HRTEM image. Titanate nanowire should be fractionized into small single crystalline grains in more rigorous conditions [13], which definitely indicates that the hydrogen titanate nanowires (Fig. 3a) should be aggregated by numerous crystalline units. The corresponding selected area electron diffraction (SAED) pattern in the inset shows some blurry spots with a ringlike distribution, which indicates the polycrystalline structure and low crystallization of nanowires.

Fig. 3c shows the sample calcined at 200 °C. It is noted that the long dislocations can be found in the direction of arrows, and the zonal crystalline areas with an average width of about 2 nm are shown between the two arrows. Lattice shears and fractures can be easily observed in this figure, and some areas without lattice fringes are also presented (note the areas in the circles). In corresponding SAED pattern, the diffraction spots are too dark to be directly captured. Therefore, the central spot was shaded in the pattern in order to give a better visibility of diffraction spots, and some blurry diffraction spots linked in lines can be observed in the inset of Fig. 3c, which indicates a disordered crystalline structure in the intermediate state of the transformation from hydrogen titanate to TiO_2-B. Associated with XRD pattern, the sample calcined at 200 °C have little peaks in 10–15°, suggesting that the layered structure of hydrogen titanate is collapsed, which may be the reason for the formation of fringe dislocations.

Fig. 4a is a HRTEM image of sample calcined at 400 °C, and circles of b–e in Fig. 4a are further magnified in Fig. 4b–e. Fig. 4a shows primary units have evolved into the larger crystalline areas, and the clear zonal dislocations grow longer in preferable

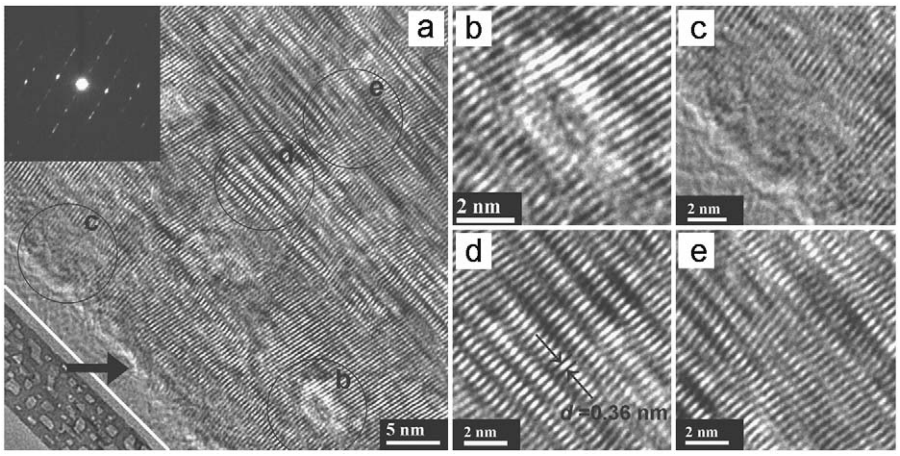

Fig. 4. HRTEM images of nanowires and SAED pattern of nanowires calcined at 400 °C.

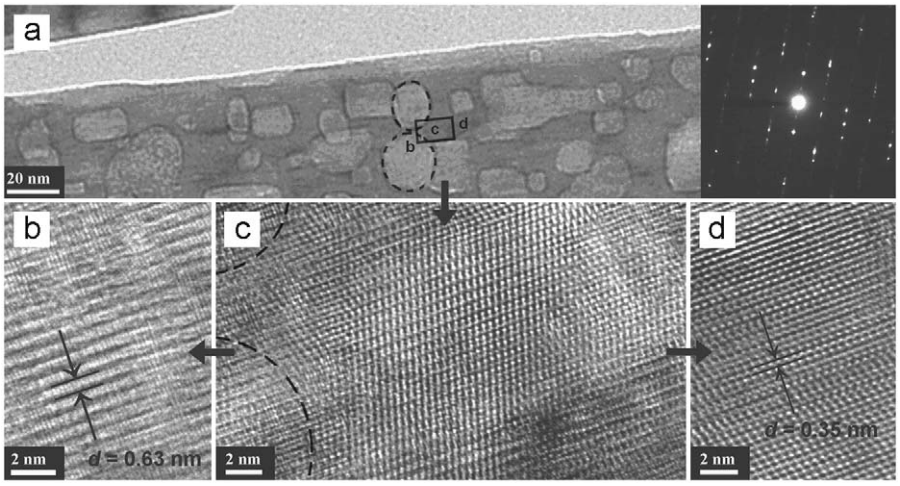

Fig. 5. HRTEM images and SAED pattern of nanowires calcined at 600 °C.

sequences. In Fig. 4b, the bigger pits have an average size of 4 nm but cannot find any lattice fringes. Some other naked areas are also presented on nanowires in Fig. 4c. The dislocations (Fig. 4d), which are vertical with the lattice fringes, can be clearly observed between the zonal crystalline areas, and the fringe spacing of 0.36 nm corresponds well to the (110) lattice planes of TiO_2-B. Lattice shears and fractures are typically shown in Fig. 4e, in which the "V-type" lattice fringes extended along two different directions. Most of the pits without lattice fringes may be developed by the rearrangement of primary crystalline units, and it is well known that the formation of the dislocation at the bonding interface was the direct consequence of the oriented attachment [16], which will be elucidated by the scheme in Fig. 6 later.

In corresponding SAED pattern, diffraction spots are linked in lines without any shade, which shows a great improvement in the crystallization of the primary crystallites. Resorted by Supplementary Information, the nitrogen adsorption–desorption isotherms and (BJH) pore size distribution measurement show that TiO_2-B nanowire calcined at 400 °C has a maximum distribution at pore size of 3.8 nm (Fig. S4, inset), and gives a S_{BET} of 36.4 $m^2 g^{-1}$, which is larger than the one ever reported under similar procedures. Furthermore, the theoretical calculated specific surface area of nanowire with a diameter size of 50 nm should be only 21.5 $m^2 g^{-1}$, showing these pits in mesoscale make great contribution to the S_{BET} of TiO_2-B nanowire [24].

Fig. 5a shows that pits on nanowires have made a further enlargement and the pore size increases to more than 10 nm at a temperature of 600 °C. Meanwhile, nanowires have eliminated the zonal dislocations and developed into larger single crystalline areas (Fig. 5c). The left side of Fig. 5c is magnified in Fig. 5b, in which lattice fringes with the distance of about 0.63 nm correspond to the (001) planes of TiO_2-B well. However, the right side of Fig. 5c is magnified in Fig. 5d, in which fringe spacings of 0.35 nm actually correspond to the (101) lattice planes of anatase. So Fig. 5c, middle section, shows the phase transformation from TiO_2-B to anatase. Additionally, it is so clear in Fig. 5a and b that the areas in pits are TiO_2-B phase and the crystalline phase of other parts on nanowires has already grown into anatase at temperature of 600 °C. The twin crystal structure, which was composed of the characteristic diffractions of TiO_2-B and anatase, was also confirmed by the diffraction spots in SAED pattern. Anatase and TiO_2-B contain chains of edge-sharing octahedral in one orientation while the other polymorphs have chains in two orientations [21]. TiO_2-B and anatase are thus structurally related so that the transformation from former to latter is a mild lattice shear which can further reduce the lattice energy.

The evolvement of pits and dislocations on TiO_2-B nanowires could be elucidated by oriented attachment mechanism. Fig. 6 is the proposed evolvement and phase transformation mechanism. The special morphology of hydrogen titanate nanowires (Fig. 6b),

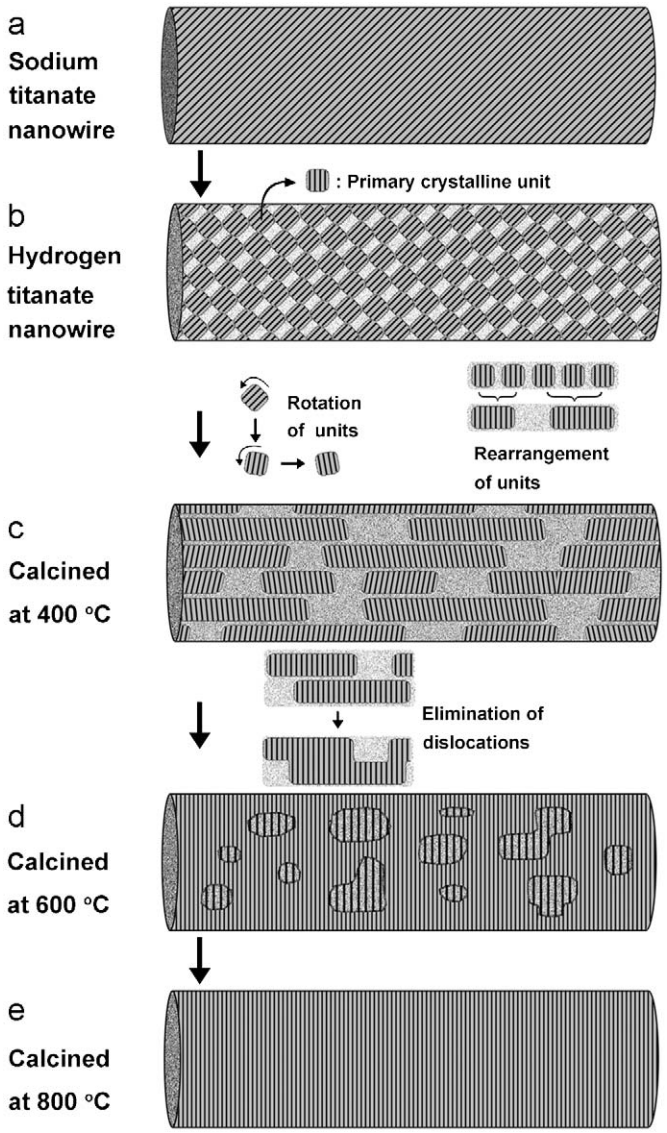

Fig. 6. The proposed evolvement mechanism of pits and dislocations on TiO_2-B nanowires.

which are accumulated by primary crystalline units, should be formed due to the upheaval of internal stress during the ion-exchange, which involves the intercalation of hydroniums and deintercalation of sodium ions. The reduction of the overall surface energy by eliminating the interface drives the oriented attachment, thus the lattice planes with higher surface energy are preferentially eliminated in the process of crystal growth [27,28]. Thus, the lattice planes (110) of TiO_2-B should be preferentially formed by the lattice distortions and rotations of primary crystalline units (Fig. 6c), during which the small fractures are partly eliminated. Therefore, the vacancies are enlarged by the rearrangement of the primary crystalline units, which leads to the formation of pits. The growth of (110) lattice planes in [110] direction is faster than the formation of other lattice planes and the extension of (110) lattice planes, which results in the formation of unique morphologies of long dislocations (Fig. 6c). Moreover, some crystalline units may rotate to the different directions, which grow into the "V-type" lattice dislocations shown in Fig. 4e.

When the highest energy interface was eliminated by oriented attachment (Fig. 6c), the subordinate high-energy interface

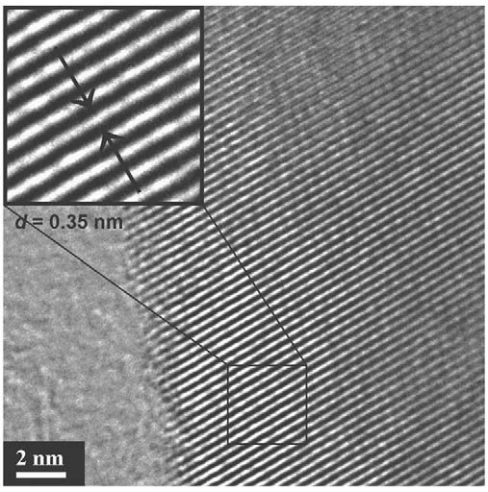

Fig. 7. HRTEM images of nanowires calcined at 800 °C.

became the highest energy interface; thus, the oriented attachment would take place sequentially on these subordinate interfaces with the increase of calcination temperature [18]. The twin crystal of TiO_2-B and anatase phase (Fig. 6d) reveals that the secondary lattice transformation arises at 600 °C. Accompanying the growth of (110) lattice planes of TiO_2-B in [110] lattice direction, the zonal crystalline areas amalgamate together to eliminate the dislocations and grow into larger single crystalline areas (Fig. 6d). Additionally, when the areas in pits grow into TiO_2-B the crystalline phase of other parts on nanowires has already become anatase at the temperature of 600 °C (Figs. 5 and 6d), which is proposed based on XRD and HRTEM results. Therefore, an intermediate state of twin crystal has been exhibited in Fig. 5. The twin crystal will grow into the single crystal of anatase at 800 °C (Fig. 6e).

The crystalline phase of sample calcined at 800 °C has completely converted into anatase, and the perfect lattice fringes without any distortions are captured by HRTEM image in Fig. 7. The square area magnified in the inset clearly shows that fringe spacings of 0.35 nm precisely correspond to the (101) lattice planes of anatase, indicating that single crystalline nanorods have been produced.

4. Conclusions

Oriented attachment growth went through the evolvement of pits and dislocations on TiO_2-B nanowires. The enlargement of the vacancies, which was caused by the rotation and rearrangement of the primary crystalline units, should be the reason of the formation of pits. The growth of (110) lattice planes in [110] direction is faster than the formation of other lattice planes and the extension of (110) lattice planes, which is the reason why unique morphologies of long dislocations come into being at 400 °C. When the growth of (110) lattice planes of TiO_2-B in [110] direction has almost finished, the zonal crystalline areas will amalgamate together to eliminate the dislocations and grow into larger single crystalline areas. So the twin crystal of TiO_2-B and anatase was exhibited at 600 °C. Finally, the anatase nanorods with the perfect lattice fringes were obtained by the elimination of pits at 800 °C.

Acknowledgments

This work was supported by the National Nature Science Foundation of China (20777015) and Shanghai Nature Science Foundation (06ZR14025).

Appendix A. Supplementary material

Supplementary data associated with this article can be found in the online version at doi:10.1016/j.jssc.2009.06.008.

References

[1] T. Kasuga, M. Hiramatsu, A. Hoson, T. Sekino, K. Niihara, Adv. Mater. 11 (1999) 1307.
[2] Q. Chen, W.Z. Zhou, G.H. Du, L.M. Peng, Adv. Mater. 14 (2002) 1208.
[3] J.G. Yu, J.C. Yu, W.K. Ho, L. Wu, X.C. Wang, J. Am. Chem. Soc. 126 (2004) 3422.
[4] Q. Wang, Z.H. Wen, J.H. Li, Adv. Funct. Mater. 16 (2006) 2141.
[5] M. Kobayashi, V.V. Petrykin, M. Kakihana, Chem. Mater. 19 (2007) 5373.
[6] Z.R. Tian, W. Tong, J.Y. Wang, N.G. Duan, V.V. Krishnan, S.L. Suib, Science 276 (1997) 926.
[7] P. Wang, S.M. Zakeeruddin, J.E. Moser, M.K. Nazeeruddin, T. Sekiguchi, M.G. Mtzel, Nat. Mater. 2 (2003) 402.
[8] G. Wang, Q. Wang, W. Lu, J.H. Li, J. Phys. Chem. B 110 (2006) 22029.
[9] Y.W. Wang, L.Z. Zhang, K.J. Deng, X.Y. Chen, Z.G. Zou, J. Phys. Chem. C 111 (2007) 2709.
[10] A.R. Armstrong, G. Armstrong, J. Canales, P.G. Bruce, Angew. Chem., Int. Ed. 43 (2004) 2286.
[11] A.R. Armstrong, G. Armstrong, J. Canales, R. Garcia, P.G. Bruce, Adv. Mater. 17 (2005) 862.
[12] T.P. Feist, P.K. Davies, J. Solid State Chem. 101 (1992) 275.
[13] L.M. Shen, N.Z. Bao, Y.Q. Zheng, A. Gupta, T.C. An, K. Yanagisawa, J. Phys. Chem. C 112 (2008) 8809.
[14] W. Sugimoto, O. Terabayashi, Y. Murakami, Y. Takasu, J. Mater. Chem. 12 (2002) 3814.
[15] J.F. Banfield, S.A. Welch, H.Z. Zhang, T.T. Ebert, R.L. Penn, Science 289 (2000) 751.
[16] R.L. Penn, J.F. Banfield, Science 287 (1998) 969.
[17] N. Du, H. Zhang, B.D. Chen, X.Y. Ma, D.R. Yang, J. Phys. Chem. C 111 (2007) 12677.
[18] H.L. Xu, W.Z. Wang, W. Zhu, L. Zhou, M.L. Ruan, Cryst. Growth Des. 7 (2007) 2720.
[19] I. Alexandrou, D.K.H. Ang, N.D. Mathur, S. Haq, G.A.J. Amaratunga, Nano Lett. 4 (2004) 2299.
[20] K.S. Cho, D.V. Talapin, W. Gaschler, C.B. Murray, J. Am. Chem. Soc. 127 (2005) 7140.
[21] J.F. Banfield, D.R. Veblen, D. Smith, J. Am. Mineral. 76 (1991) 343.
[22] R. Yoshida, Y. Suzuki, S. Yoshikawa, J. Solid State Chem. 178 (2005) 2179.
[23] R. Ma, Y. Bando, T. Sasaki, J. Phys. Chem. B 108 (2004) 2115.
[24] S. Pavasupree, Y. Suzuki, S. Yoshikawa, R. Kawahata, J. Solid State Chem. 178 (2005) 3110.
[25] Y. Suzuki, S. Pavasupree, S. Yoshikawa, R. Kawahata, J. Mater. Res. 20 (2005) 1063.
[26] ICDD-JCPDS database, #46-1238 (TiO_2-B).
[27] R.L. Penn, J.F. Banfield, Geochim. Cosmochim. Acta 63 (1999) 1549.
[28] H.L. Xu, W.Z. Wang, W. Zhu, Chem. Lett. 35 (2006) 264.